Pediatric Optical Coherence Tomography in Clinical Practice—Recent Progress

Helena Lee,[1,2] Frank A. Proudlock,[2] and Irene Gottlob[2]

[1]Clinical and Experimental Sciences, Faculty of Medicine, University of Southampton, Southampton, United Kingdom
[2]University of Leicester Ulverscroft Eye Unit, Leicester, United Kingdom

PURPOSE. Optical coherence tomography (OCT) has revolutionized the diagnosis and management of adult retinal and optic nerve disease. Children were deprived of this technology until the recent development of handheld spectral-domain OCT (HH-SDOCT). In this article, we review the applications of OCT imaging in pediatric ophthalmology.

METHODS. This study was a review of the literature.

RESULTS. The acquisition and interpretation of pediatric tomograms differ significantly from those for adults, with adjustments needed to account for the shorter axial lengths, higher refractive errors, and ongoing retinal and optic nerve development in the pediatric eye. Handheld SDOCT is increasingly being used as an adjunctive diagnostic tool in retinopathy of prematurity (ROP) and nonaccidental injury (NAI) by providing additional morphologic information that is not normally clinically discernible. The role of HH-SDOCT in streamlining diagnosis in infantile nystagmus syndrome, retinal dystrophies, and degenerations has been established. Optical coherence tomography can also help differentiate between pediatric intraocular tumors, for example, hamartomas and retinoblastoma; monitor tumor progression; and monitor treatment response. In addition, HH-SDOCT is establishing its role as a noninvasive monitoring tool in children affected by optic nerve pathology such as glaucoma, optic nerve atrophy and hypoplasia, optic pathway glioma, and pseudotumor cerebri.

CONCLUSIONS. Handheld SDOCT can provide novel insights into the natural history of retinal and optic nerve diseases in young children. For example, in achromatopsia and albinism, in vivo OCT studies have provided evidence of altered but ongoing retinal development in early childhood, which suggests that potentially targeting treatment at an earlier age may optimize visual function by normalizing retinal development.

Keywords: optical coherence tomography, retinal development, children's vision

Optical coherence tomography (OCT) is a diagnostic imaging technique that provides cross-sectional images of human retinal morphology in vivo. Optical coherence tomography has revolutionized the diagnosis and treatment of adults with retinal disease.[1–3] Until recently, infants and young children were deprived of this technology. The reason for this is that conventionally, OCT imaging is a chin rest system that requires good fixation and cooperation, thus limiting its use in infants and young children. A handheld spectral-domain OCT (HH-SDOCT), which has been developed and optimized for use in the pediatric population, has overcome these limitations and has been shown to be reliable.[4–7]

There are multiple applications for the HH-SDOCT, including: (1) imaging infants with retinopathy of prematurity (ROP) or other retinal disorders, (2) investigating nystagmus and trauma, and (3) diagnosis and monitoring of intraocular tumors and optic nerve disease.[8–10] Handheld SDOCT can also identify retinal manifestations of systemic disease, for example, the presence of retinal edema in neonatal hemochromatosis and liver failure or retinal thinning in cobalamin C type methylmalonic aciduria with homocystinuria.[11,12]

CHALLENGES AND PECULIARITIES OF PEDIATRIC OCT IMAGING

The biometric properties of the infant human eye are significantly different in comparison to those of adults, with shorter axial lengths, steeper corneal curvatures, and greater astigmatism and refractive errors.[4] Preterm infants are predominately myopic, the degree of which decreases with increasing age until there is a shift to hyperopia by approximately 40 to 52 weeks.[13,14] Age-specific adjustments in the OCT imaging protocol need to be established in order to ensure optimal image acquisition in young children. Normally, an OCT scan of the retina is obtained by pivoting the OCT beam in the iris plane. In the shorter infant eye, the OCT scanning pivot position is anterior to the iris plane, resulting in clipping of the peripheral portion of the image by the iris.[4] The shorter axial length may be corrected for by shortening the OCT reference arm position such that the pivot point is positioned in the iris plane.[4] The image is further optimized by adjusting the focus of the handheld probe (range, −10 to +12 diopters) to correct for any refractive errors.[4] In addition, the shorter axial length of the infant human eye results in a magnified retinal image, which alters the scan position on the retina relative to an eye with a
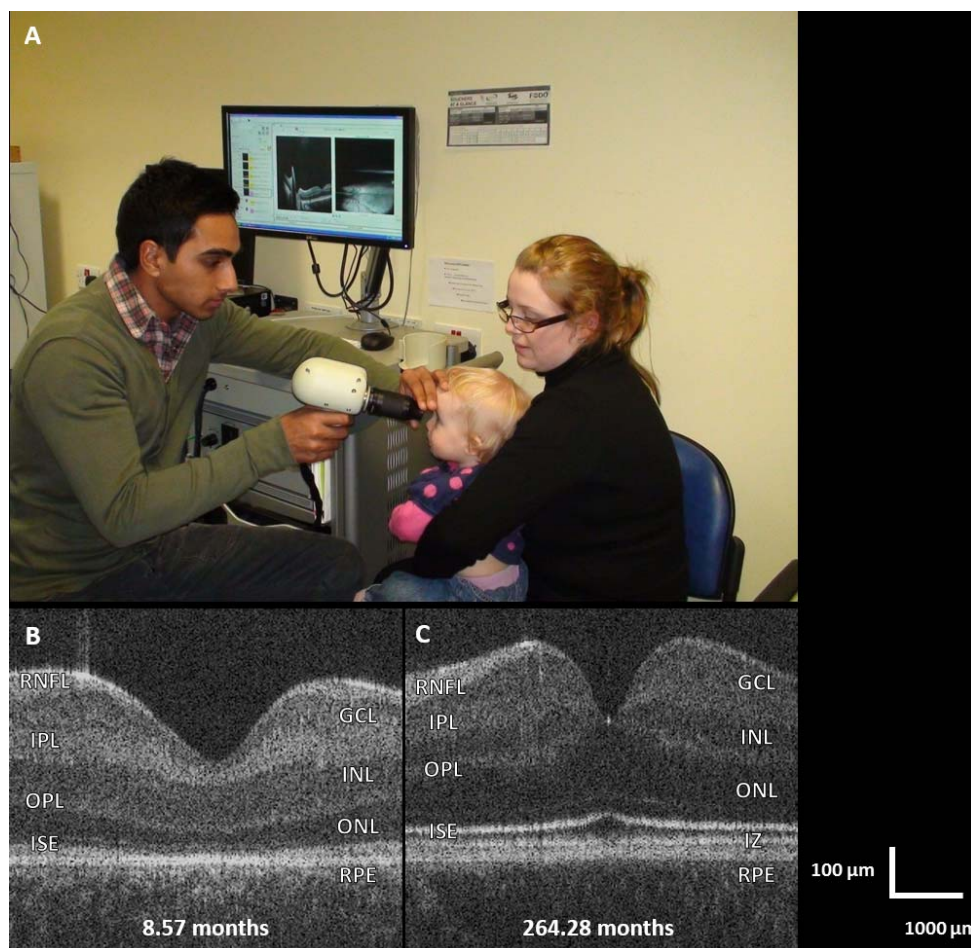
FIGURE 1. **(A)** Example of using HH-SDOCT to acquire a retinal tomogram in a child and two foveal tomograms taken at the foveal center illustrating normal retinal anatomy and the morphologic differences between the neonatal (**B**) and adult retina (**C**). Both participants were born at term, and the ages of the participants are given in months postmenstrual age. During normal foveal development, there is migration of the IRLs (GCL, IPL, INL, and OPL) away from the central fovea, migration of the cone photoreceptors into the central fovea, and elongation of the ORLs (ONL, IS, and OS) with increasing age. This explains the presence of the IRLs and absence of cone photoreceptors at the central fovea on the neonatal OCT (**B**). In contrast, the IRLs are absent and the cone photoreceptors are present at the central fovea on the adult OCT (**C**). The presence of the interdigitation zone in (**C**) is an additional marker of retinal maturity.

longer axial length.[15] In order to facilitate comparisons at specific locations across different age groups, the lateral scales for the OCT data need to be adjusted based on age-specific axial length estimates.[4]

Images obtained using the handheld probe may also contain movement artifacts caused by the examiner and/or the child.[8,16] Therefore, HH-SDOCT imaging is limited by its lack of automatic registration for serial measurements, and it may be prudent to consider conventional table-based SDOCT imaging in older children who are sufficiently cooperative. The importance of a child-friendly environment in maximizing cooperation from infants and young children undergoing HH-SDOCT imaging should not be underestimated. Children are much more at ease in a private, spacious, and imaginatively decorated environment that is easy to navigate and in which there is control over noise and lighting. Access to information and communications technology is also suggested.[17] In our experience, we have found that a variety of techniques can be used in order to keep children calm and cooperative for OCT examination. Optical coherence tomography scanning of young infants was most often successful if acquired when the child was seated on a parent's lap while bottle feeding or breastfeeding. Optical coherence tomography imaging could also be successfully carried out with an infant lying supine in

his or her own pram or stroller, particularly if infants were drowsy at the time of imaging. Less than 10% of children younger than 12 months of age were imaged lying supine. Children older than 12 months of age responded well to animated fixation targets, for example, age-appropriate cartoons that were employed using a portable laptop computer, which was positioned behind the examiner (Fig. 1A).

CONSIDERATIONS WHEN INTERPRETING PEDIATRIC OCT IMAGING

The bands identified on OCT imaging obtained at different ages ranging from 30 weeks gestational age (GA) to 65 years have been correlated with major histologic findings obtained from a range of eyes aged between 22 weeks GA to 72 years, validating OCT as a reliable quantitative tool in assessing foveal morphology (Fig. 1B).[18–20] In addition, it is important to consider the corrected age of the child when assessing foveal morphology on OCT, as there are age-related variations in both the appearances and measurements of each retinal layer due to ongoing foveal development.[21]

Normal foveal development continues until early adolescence and is associated with unique developmental trajectories

for each individual retinal layer (Fig. 2).[21] It is a complex process, involving centrifugal migration of the inner retinal layers (IRLs), retinal nerve fiber layer (RNFL), ganglion cell layer (GCL), inner plexiform layer (IPL), inner nuclear layer (INL), and outer plexiform layer (OPL) away from the central fovea, as well as centripetal migration of the cone photoreceptors into the central fovea and elongation of the outer retinal layers (ORLs), outer nuclear layer (ONL), and photoreceptor inner (IS) and outer (OS) segments with increasing age (Fig. 2).[5,20-22]

As a consequence, some of the bands that are normally visualized on adult tomograms, including the ellipsoid band of the photoreceptor inner segments (ISE), external limiting membrane (ELM), and interdigitation zone (IZ), are often absent on tomograms taken from premature and younger term infants (Fig. 1B).[5,20,21] There is variability in the timing of when the ISE, OS, and IZ bands all become visible in the central fovea on OCT imaging.[5,20,21,23] In general, the IZ band is the last band to mature and is almost never visualized prior to 46 to 47 weeks GA.[5,20,21] Pediatric normative reference data for each retinal layer have been reported for children aged between birth and 17 years of age, which may help in the diagnosis and monitoring of pediatric retinal disease.[21,24-26]

Similarly, interpretation of pediatric optic nerve morphology on OCT also requires consideration of GA. Significant differences in early optic nerve development and morphology have been observed in preterm infants as compared to term infants, including thinning of the superior, nasal, and inferior peripapillary RNFL and a larger vertical disc diameter (vDD) (908 vs. 700 μm) and cup-to-disc ratio (vCDR) (0.68 vs. 0.53 μm).[27,28] As the optic nerve develops in preterm infants, there is an increase in the vDD and a decrease in vCDR.[28] Peripapillary RNFL measurements are known to be thicker in children than in adults.[29] As a result, previously established adult reference OCT data cannot be used in the diagnosis and monitoring of pediatric optic nerve disease. Normative reference RNFL data have been reported for children aged between birth and 17 years of age, which may help in the interpretation of pediatric optic nerve OCT imaging.[25,26,29-33]

RETINOPATHY OF PREMATURITY

Retinopathy of prematurity is one of the leading and preventable causes of childhood blindness worldwide.[34] Retinopathy of prematurity is known to alter development of the central retina and is associated with high refractive errors and deficits in visual acuity and sensitivity.[35-42] In children with a history of ROP, there is persistence of the foveal IRLs, reduction of foveal pit depth, reduction in the diameter of the foveal avascular zone (FAZ), increase in central macular thickness (CMT) measurements, thinning of the GCL-IPL complex, delay in photoreceptor development, and thinning of the photoreceptor layers.[5,38-55] Optic nerve morphology is altered in preterm children, with global decreases and segmental (temporal) increases in RNFL thickness measurements being reported.[27,53,56,57] Choroidal thickness, which normally increases with age, is reduced in preterm children.[45,50,58-60] Iridocorneal angle development and morphology are also affected, with evidence of a wider angle, a more convex iris configuration, and a shallower anterior chamber depth.[50,61]

Handheld SDOCT may be a useful adjunct to binocular indirect ophthalmoscopy screening in ROP.[62] Using HH-SDOCT, subclinical findings such as preretinal tissue (popcorn retinopathy), epiretinal membranes, cystoid macular edema (CME), retinal layer schisis, precise localization of retinal detachment, vascular abnormalities, and foveal architectural abnormalities not visible on conventional clinical examination can be identified.[62-66]

A number of HH-SDOCT-based morphologic features are being investigated as potential prognostic indicators in ROP. Cystoid macular edema has been reported to be present in up to 46.3%, 57.1%, and 87.5% of eyes affected by stage 1, 2, and 3 ROP, respectively.[5,13,23,51,67-69] The presence of CME is associated with higher hyperopia and poorer neurodevelopmental and visual acuity outcomes.[70-72] A vascularity abnormality (VASO) score has been described that appears to be significantly higher in eyes with plus disease (Fig. 3).[73] Increased central foveal, IRL, and foveal to parafoveal retinal thickness measurements are associated with a higher risk of developing plus disease or ROP stage 3 and requiring laser treatment (Fig. 4).[74]

NONACCIDENTAL INJURY OR TRAUMA

Handheld SDOCT is helpful in the evaluation of nonaccidental injury (NAI) by identifying previously unrecognized vitreoretinal abnormalities including posterior vitreous separation and multilayered retinoschisis.[75] It has been used to guide treatment in infants with shaken baby syndrome by providing additional morphologic information.[67] Using this information, decisions were made not to proceed with macular hole surgery in one infant with signs of chronic retinal changes and to perform additional epiretinal membrane (ERM) peel in a second infant, which resulted in an excellent postoperative visual outcome.

RETINAL DYSTROPHIES, DYSPLASIAS, AND INFANTILE NYSTAGMUS

Handheld SDOCT is being used to characterize and monitor retinal dystrophies, dysplasias, and degenerations that present in early childhood, for example, foveal hypoplasia in albinism,[16] disruption of photoreceptor integrity in Bardet-Biedl syndrome,[76] retinal dysplasia in Walker-Warburg syndrome,[77] and X-linked retinoschisis (Fig. 5).[78] In particular, HH-SDOCT has been shown to be very helpful in identifying the etiology of infantile nystagmus syndrome (INS) (a heterogeneous group of disorders, for which there are multiple causes with different prognoses).[16,79]

A HH-SDOCT diagnostic algorithm has been developed that streamlines the investigation of infants and young children with nystagmus.[79] Through the identification of the presence or absence of typical or atypical foveal hypoplasia (presence of the normally absent IRLs at the fovea) and the presence of other abnormal morphologic features, it is possible to divide INS into four diagnostic categories—typical foveal hypoplasia, atypical foveal hypoplasia, abnormal foveal morphology, and normal foveal morphology—and focus further investigations (Fig. 6).[79] In this way, conditions such as albinism and PAX6 mutations that are usually associated with typical foveal hypoplasia can be distinguished from other conditions such as achromatopsia (ACHM), which is characterized by atypical foveal hypoplasia (foveal hypoplasia associated with photoreceptor disruption and/or the presence of hyperreflective zone located between the ELM and RPE at the fovea), or retinal dystrophies, which are typically associated with abnormal lamination of the IRLs and ORLs, loss or disruption of photoreceptor integrity, and thinning of the ONL and RPE.[79]

Using the HH-SDOCT to investigate in vivo retinal development in infants and young children affected by ACHM and albinism has provided some novel and important insights into the natural history of these conditions.[80,81] In ACHM,
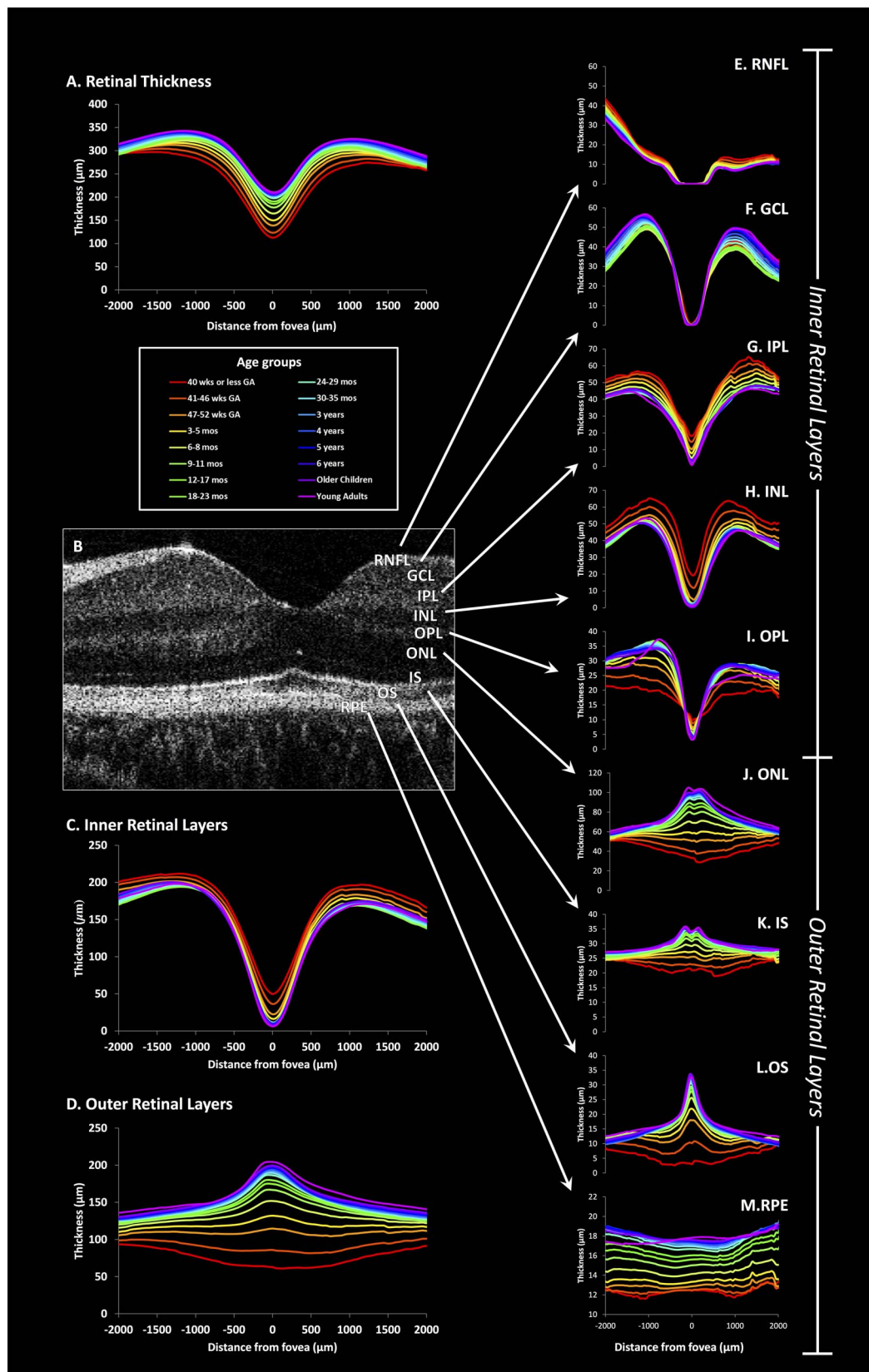
FIGURE 2. Summary of the development of each retinal layer over time. The mean thickness of each retinal layer plotted using a fourth-order polynomial fit for 261 participants aged between 8.4 and 333.9 months corrected age who were divided into 16 color-coded age groups. In this figure, the acronym GA refers to the corrected age of the participants, which was calculated by adding the gestational age (total time in utero) to the chronological age (based on birth date). All participants were born at term. Reprinted with permission from Lee H, Purohit R, Patel A, et al. In vivo foveal development using optical coherence tomography. *Invest Ophthalmol Vis Sci.* 2015;56:4537–4545. © 2015 Association for Research in Vision and Ophthalmology.
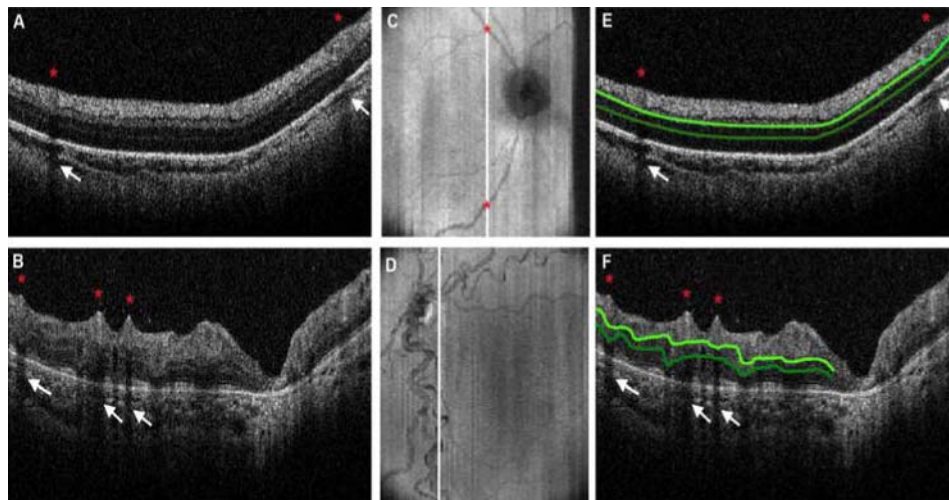
FIGURE 3. Handheld SDOCT scans from a 31-week PMA neonate ROP zone II, stage 2, and no plus disease (**A**) and a 48-week PMA neonate, ROP zone II, stage 3, and plus disease (**B**). The vascularity abnormality (VASO) score is based on four characteristics: retinal vessel elevation (**B**); scalloped retinal layers (**F**); hyporeflective vessels; and retinal spaces. Reprinted with permission from Maldonado RS, Yuan E, Tran-Viet D, et al. Three-dimensional assessment of vascular and perivascular characteristics in subjects with retinopathy of prematurity. *Ophthalmology.* 2014;121:1289–1296. © 2014 American Academy of Ophthalmology.

there is evidence that retinal development is not arrested but is ongoing, albeit at a reduced rate and magnitude in comparison to controls.[80] This manifests as foveal hypoplasia, and reductions in ORL thickness, total retinal thickness, and parafoveal IRL, IPL, and OPL thickness measurements.[80] Of particular note, ACHM appears to be a much more dynamic condition in infants and young children in comparison to adults, with ongoing changes in the degree of photoreceptor disruption observed on longitudinal follow-up.[80]

Similarly, longitudinal OCT imaging studies in albinism have demonstrated that retinal development is ongoing in early childhood, although reduced in rate and magnitude in comparison to controls, resulting in foveal hypoplasia and a reduction in ORL thickness measurements.[81] In contrast to ACHM, the CMT is significantly increased in comparison to controls.[81] Interestingly, there is an initial decrease in CMT in early infancy in albinism as a result of ongoing regression of the IRLs from the fovea.[81] This suggests that there is a period of retinal developmental plasticity in childhood in both ACHM and albinism. Potentially, targeting treatment to the earlier

stages of these conditions may help normalize retinal development and optimize vision.

Ocular Oncology

Optical coherence tomography potentially has a role in differentiating between various pediatric intraocular tumors such as combined hamartoma of the retina and RPE (CHRRPE), astrocytic hamartomas, and retinoblastoma, which can be achieved through a systematic evaluation of tumor reflectivity, degree of involvement of individual retinal layers, associated vitreoretinal interface abnormalities, and the transition pattern between abnormal and normal retina.[10,82–89]

Combined hamartoma of the retina and RPE appears as a hyperreflective mass on OCT, with thickening and disorganization of the IRLs and an overlying ERM associated with traction and retinal folds.[82,86] In contrast, astrocytic hamartomas appear as a hyperreflective mass localized to the RNFL associated with optically empty spaces, focal vitreous adhesions, and a gradual transition between tumor and surrounding
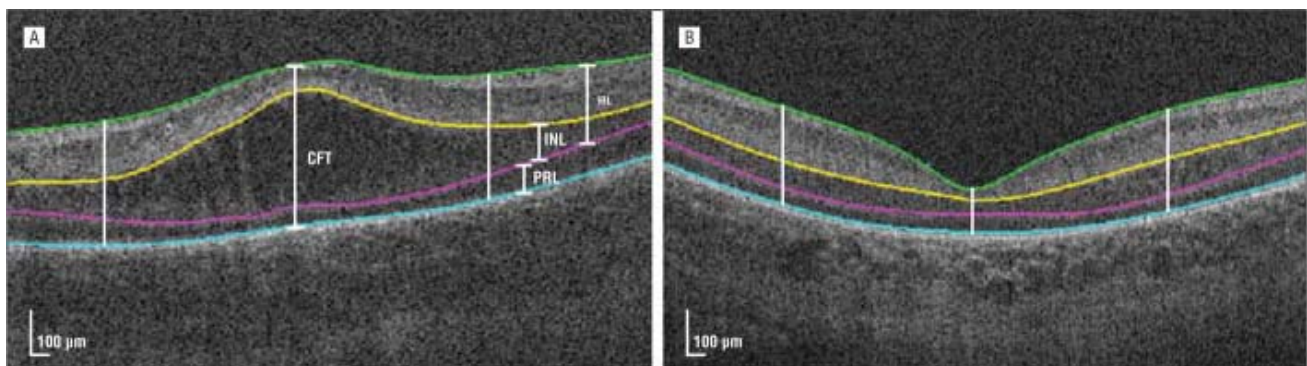

FIGURE 4. Handheld SDOCT scans from two premature infants: one with edema (**A**) and one without edema (**B**). The foveal-to-parafoveal (FP) thickness ratio provides a quantitative measure of foveal contour and is calculated by dividing the central foveal thickness (CFT) by an average of the retinal thickness values at 1000 μm on either side of the fovea (*white parafoveal vertical bars*). Reprinted with permission from Maldonado RS, O'Connell R, Ascher SB, et al. Spectral-domain optical coherence tomographic assessment of severity of cystoid macular edema in retinopathy of prematurity. *Arch Ophthalmol.* 2012;130:569–578. © 2012 American Medical Association. All rights reserved.
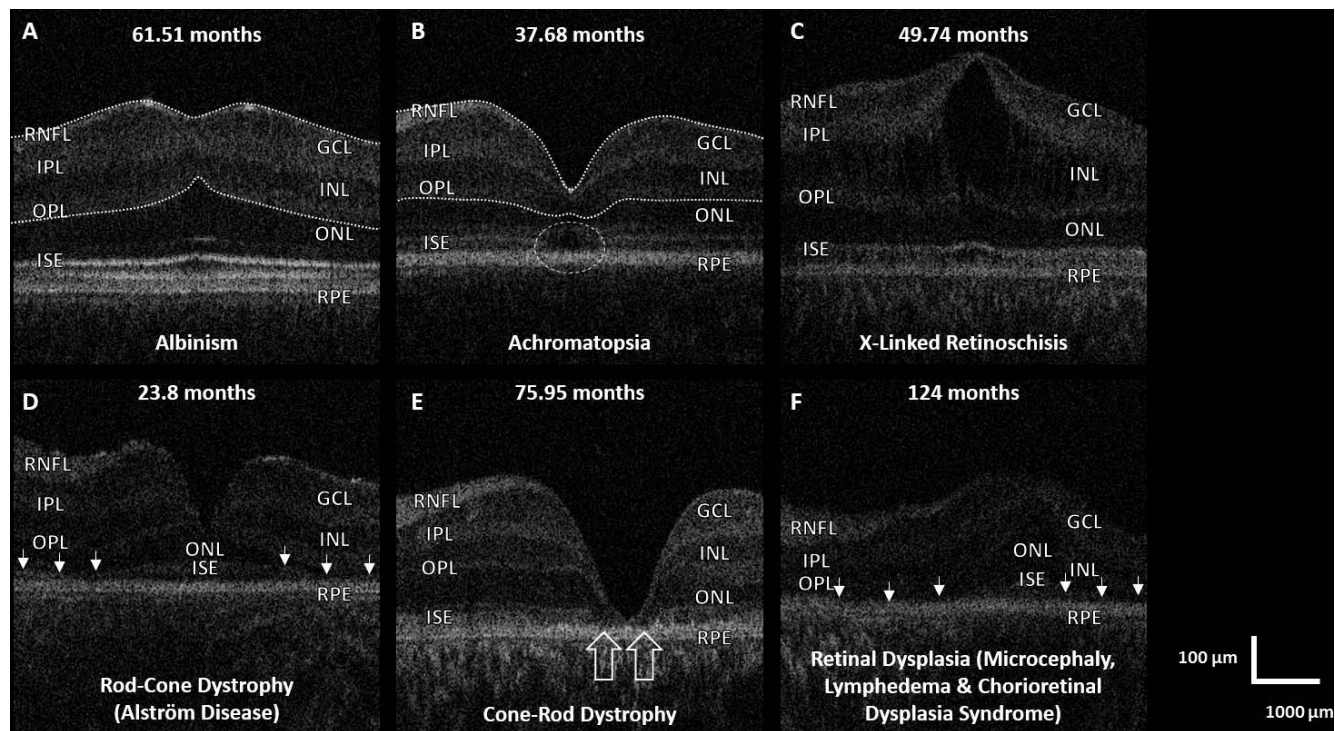
FIGURE 5. Foveal tomograms obtained from children, which demonstrate some of the characteristic features seen with retinal dystrophies, dysplasias, or infantile nystagmus on OCT imaging. (**A**) Typical foveal hypoplasia, where there is continuation of the normally absent IRLs (*outlined in white*) in a case of albinism. (**B**) Atypical foveal hypoplasia in achromatopsia, where in addition to foveal hypoplasia (IRLs *outlined in white*), there is ISE disruption and a hyporeflective zone (*white circle*). (**C**) Split in the inner nuclear layer in a case of X-linked retinoschisis. (**D**) Absent rod photoreceptors and ISE (*small white arrows*) and ONL thinning in a case of rod–cone dystrophy associated with Alström syndrome. (**E**) Absent cone photoreceptors and thinning of the ONL (*empty arrows*) in a case of cone–rod dystrophy. (**F**) Retinal dysplasia consisting of absent rod photoreceptors and ISE (*small white arrows*), ONL thinning, and abnormal lamination of the inner retinal layers seen in a case of microcephaly lymphedema and chorioretinal dysplasia.

normal tissue.[84,85] Retinoblastoma lesions appear isodense or hyperdense on OCT, are associated with patches of calcification, and usually have an abrupt transition toward uninvolved retina, which helps to distinguish them from hamartomas (Fig. 7).[10,84] The degree of retinal layer involvement is dependent on lesion size, which extends from involvement of the inner nuclear and middle retinal layers in isolation with preservation of the RNFL and ORLs (smaller tumors), to involvement of the full thickness of the retina (larger tumors).[10] Preretinal seeds in retinoblastoma are located superficial to the retina, appear isodense and smooth, and are associated with shadowing of the underlying structures on OCT.[10] Optical coherence tomography is also proving useful with regard to monitoring tumor progression, identifying new lesions and recurrences, monitoring treatment response, and guiding further management.[10,82–90]

OPTIC NERVE PATHOLOGY

Optical coherence tomography is beginning to establish itself as a diagnostic and monitoring tool with regard to pediatric optic nerve pathology, including conditions such as: glaucoma, optic nerve atrophy, optic nerve hypoplasia, optic pathway glioma, pseudotumor cerebri and optic nerve pits (Fig. 8). It can distinguish between glaucomatous and nonglaucomatous optic atrophy in children, with INL cysts, CME, outer retinal and photoreceptor loss, total retinal atrophy, pigment epithelial detachment with associated subretinal fluid, choroidal folds, and ISE disruption more likely to be present in the latter.[91] Optical coherence tomography may potentially serve

as a noninvasive monitoring tool in pediatric glaucoma with evidence that RNFL and macular thickness measurements decrease with increasing grade of glaucomatous damage.[92]

In primary congenital and juvenile open-angle glaucoma, OCT is being used to investigate RNFL thickness and cupping reversal in response to surgical intervention and is providing novel insights into the natural history of pediatric glaucoma.[93] Although cupping reversal has generally been considered a marker of successful treatment outcome, recent work suggests that this may not be the case and that the preoperative cupping observed in pediatric glaucoma reflects true RNFL damage rather than a change in optic nerve compliance.[94] Interestingly, the preoperative optic nerve head cup-to-disc ratio (CDR) may be a better predictor of postoperative RNFL thickness.[93]

Handheld SDOCT has also been used to investigate optic nerve and retinal morphology in children with optic nerve hypoplasia. In addition to significantly smaller discs, horizontal cup diameters, and cup depths, some interesting and novel alterations in macular morphology have been characterized, including foveal hypoplasia and thinning of the RNFL, GCL, IPL, ONL, and IS.[95]

Optical coherence tomography also can detect RNFL loss from optic atrophy occurring secondary to optic pathway glioma in older children affected by neurofibromatosis type 1.[96] In addition, the potential of the HH-SDOCT to monitor progressive optic neuropathies such as optic nerve glioma in infants and young children unable to cooperate with traditional OCT testing devices has been established.[97] It has been demonstrated that measurements of the RNFL, GCL, and IPL
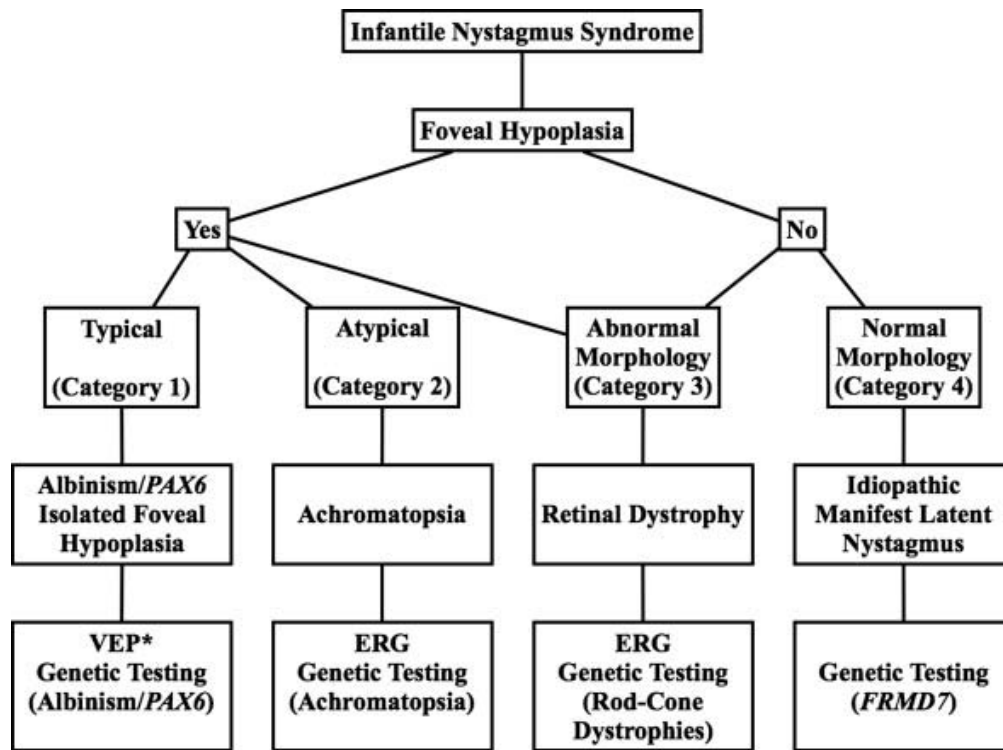
FIGURE 6. Algorithm for the diagnosis of infantile nystagmus syndrome on the basis of OCT findings. Depending on the presence or absence of foveal hypoplasia or the presence or absence of other abnormal macular morphology, the etiology of nystagmus can be predicted and diagnostic tests can be selected to confirm the diagnosis. Reprinted with permission from Lee H, Sheth V, Bibi M, et al. Potential of handheld optical coherence tomography to determine cause of infantile nystagmus in children by using foveal morphology. *Ophthalmology.* 2013;120:2714–2724. © 2013 American Academy of Ophthalmology.

thickness can discriminate between children with and without vision loss from their optic nerve pathway gliomas, thus suggesting that HH-SDOCT can be used as a surrogate marker of visual function in infants and young children.[96,98]

Similarly, OCT can be used to diagnose and monitor pediatric pseudotumor cerebri and is potentially useful as a visual prognostic tool in this condition.[99,100] An increased central macular, temporal, and superior RNFL thickness has been described in children affected by pseudotumor cerebri.[101] The presence of optic atrophy and photoreceptor loss on OCT in pseudotumor cerebri are findings that are highly associated with irreversible visual loss.[100]

Interestingly, optic nerve parameters may also be predictive of central nervous system development and pathology, with larger vCDR being associated with lower Bayley Scales of Infant Development scores.[28,33] A weak association has been described between a larger vertical cup diameter (vCD) and vCDR with periventricular leukomalacia, and a shallower cup with posthemorrhagic hydrocephalus.

DISCUSSION AND CONCLUSIONS

Pediatric OCT imaging is a rapidly expanding area that is revolutionizing the diagnosis and management of pediatric retinal and optic nerve diseases. The interpretation of pediatric OCT is a complex art, as one is often observing the effects of disease in the setting of ongoing retinal and optic nerve development in young children. The provision of normative developmental OCT data will help facilitate age-specific interpretation of pediatric OCT imaging.

Optical coherence tomography has demonstrated its potential as an objective and noninvasive diagnostic and monitoring tool in infants and young children with ROP, NAI, retinal dystrophies, infantile nystagmus, ocular oncology, glaucoma, and pseudotumor cerebri. These conditions are often difficult to diagnose and manage in infants and young children due to the limited ability of this age group to cooperate with standard adult diagnostic and monitoring tools. The incorporation of pediatric OCT imaging into the clinical assessment of pediatric retinal and optic nerve diseases is providing additional information that is assisting in management decisions. For example, several OCT measures are emerging as surrogate markers of visual acuity in optic nerve glioma (RNFL, GCL, and IPL thickness) and pseudotumor cerebri (RNFL thickness). It would be interesting to investigate if these or other OCT measures of visual acuity/function can be extended to other pediatric retinal and optic nerve diseases.

One area of pediatric ophthalmology in which the application(s) of OCT has been most investigated is ROP, where it is being used as an adjunct to binocular indirect ophthalmoscopy to provide additional information to aid in the earlier diagnosis, monitoring, and treatment of ROP. The presence of CME and altered foveal architectural and optic nerve parameters has been shown to predict visual and neurodevelopmental outcomes in ROP. It would be interesting to investigate whether these parameters can be used as universal predictors of visual and neurodevelopmental outcomes in other pediatric retinal and optic nerve diseases, as well as whether integration of OCT imaging into ROP screening results in improved structural and functional outcomes for infants with ROP in the long term.

Finally, the ability to perform in vivo OCT investigation of retinal and optic nerve diseases in infants and young children
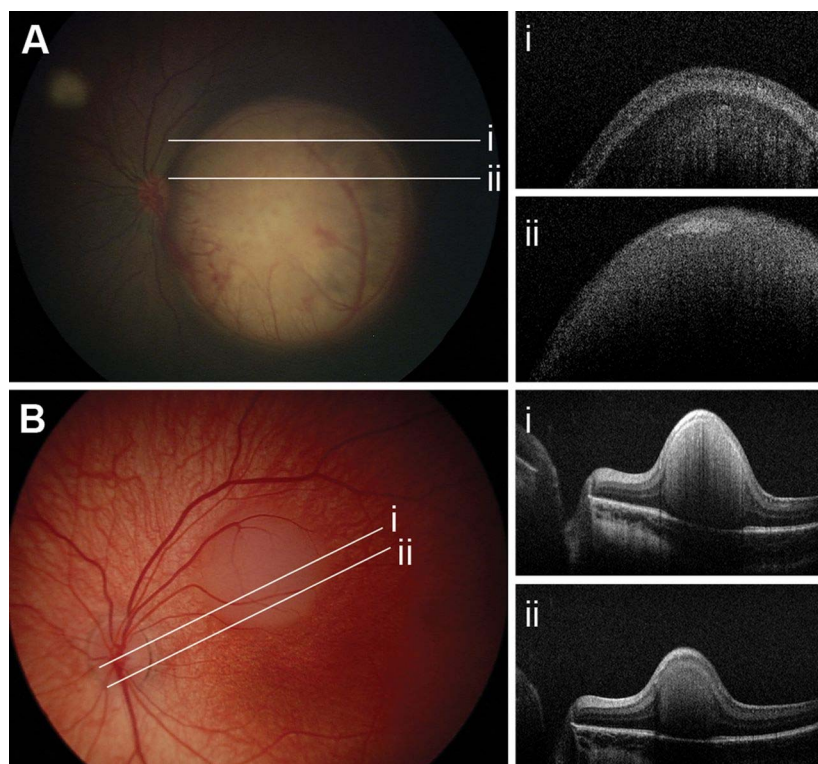
FIGURE 7. RetCam and HH-SDOCT images of two medium-sized retinoblastoma tumors located at the macula (**A**) and superior arcade (**B**). The retinoblastoma tumors appear isodense on OCT and are clearly demarcated from the surrounding healthy retina. The inner retinal layers are relatively uninvolved in these images. Reprinted with permission from Rootman DB, Gonzalez E, Mallipatna A, et al. Hand-held high-resolution spectral domain optical coherence tomography in retinoblastoma: clinical and morphologic considerations. *Br J Ophthalmol*. 2013;97:59–65. Copyright © 2013 BMJ Publishing Group Ltd.

has provided some important insights into the natural history of conditions such as achromatopsia and albinism early in life. These conditions appear much more dynamic in children than in adults, which suggests that retinal disease in early childhood is a process that results in abnormal retinal development as opposed to retinal degeneration. It would be interesting to investigate if retinal and optic nerve development are similarly affected in other conditions in order to increase our understanding of both normal and abnormal retinal and optic nerve development and identify novel therapeutic targets. Potentially,
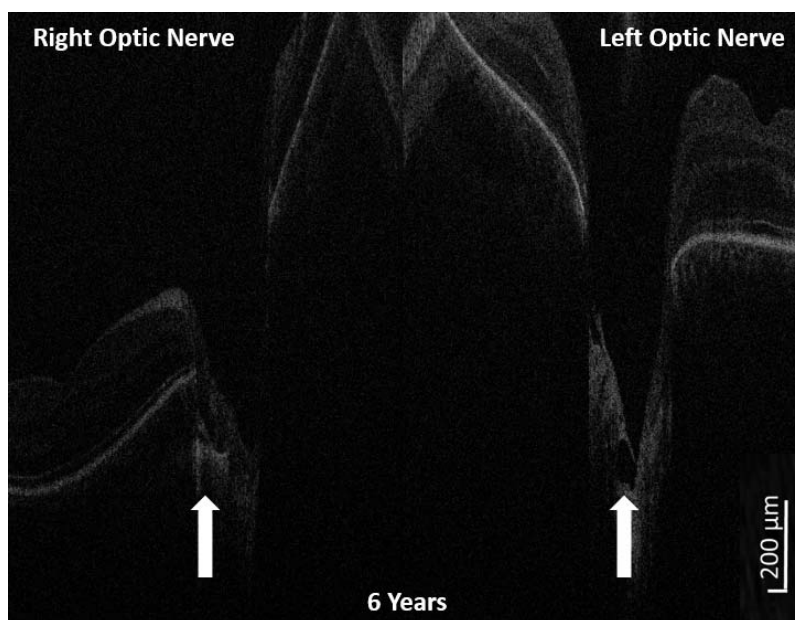

FIGURE 8. Handheld SDOCT images of bilateral optic disc pits (*white arrows*) in a 6-year-old child.

targeting treatments to this critical period of plasticity in children may be the key to maximizing visual function through normalizing retinal and optic nerve development.

References

1. Schuman SG, Koreishi AF, Farsiu S, et al. Photoreceptor layer thinning over drusen in eyes with age-related macular degeneration imaged in vivo with spectral-domain optical coherence tomography. *Ophthalmology*. 2009;116:488–496, e2.

2. Forooghian F, Cukras C, Meyerle CB, et al. Evaluation of time domain and spectral domain optical coherence tomography in the measurement of diabetic macular edema. *Invest Ophthalmol Vis Sci*. 2008;49:4290–4296.

3. Han IC, Jaffe GJ. Comparison of spectral- and time-domain optical coherence tomography for retinal thickness measurements in healthy and diseased eyes. *Am J Ophthalmol*. 2009; 147:847–858, e1.

4. Maldonado RS, Izatt JA, Sarin N, et al. Optimizing hand-held spectral domain optical coherence tomography imaging for neonates, infants, and children. *Invest Ophthalmol Vis Sci*. 2010;51:2678–2685.

5. Maldonado RS, O'Connell RV, Sarin N, et al. Dynamics of human foveal development after premature birth. *Ophthalmology*. 2011;118:2315–2325.

6. Lee H, Proudlock F, Gottlob I. Is handheld optical coherence tomography reliable in infants and young children with and without nystagmus? *Invest Ophthalmol Vis Sci*. 2013;54:8152–8159.

7. Avery RA, Cnaan A, Schuman JS, et al. Intra- and inter-visit reproducibility of ganglion cell-inner plexiform layer measurements using handheld optical coherence tomography in children with optic pathway gliomas. *Am J Ophthalmol*. 2014;158:916–923.

8. Gerth C, Zawadzki RJ, Heon E, et al. High-resolution retinal imaging in young children using a handheld scanner and Fourier-domain optical coherence tomography. *J AAPOS*. 2009;13:72–74.

9. Maldonado RS, Toth CA. Optical coherence tomography in retinopathy of prematurity: looking beyond the vessels. *Clin Perinatol*. 2013;40:271–296.

10. Rootman DB, Gonzalez E, Mallipatna A, et al. Hand-held high-resolution spectral domain optical coherence tomography in retinoblastoma: clinical and morphologic considerations. *Br J Ophthalmol*. 2013;97:59–65.

11. Maldonado RS, Freedman SF, Cotten CM, et al. Reversible retinal edema in an infant with neonatal hemochromatosis and liver failure. *J AAPOS*. 2011;15:91–93.

12. Fuchs LR, Robert M, Ingster-Moati I, et al. Ocular manifestations of cobalamin C type methylmalonic aciduria with homocystinuria. *J AAPOS*. 2012;16:370–375.

13. Cook A, White S, Batterbury M, et al. Ocular growth and refractive error development in premature infants with or without retinopathy of prematurity. *Invest Ophthalmol Vis Sci*. 2008;49:5199–5207.

14. Gordon RA, Donzis PB. Refractive development of the human eye. *Arch Ophthalmol*. 1985;103:785–789.

15. Sanchez-Tocino H, Alvarez-Vidal A, Maldonado MJ, et al. Retinal thickness study with optical coherence tomography in patients with diabetes. *Invest Ophthalmol Vis Sci*. 2002; 43:1588–1594.

16. Chong GT, Farsiu S, Freedman SF, et al. Abnormal foveal morphology in ocular albinism imaged with spectral-domain optical coherence tomography. *Arch Ophthalmol*. 2009;127: 37–44.

17. Lambert V, Coad J, Hicks P, et al. Young children's perspectives of ideal physical design features for hospital-built environments. *J Child Health Care*. 2013;18:57–71.

18. Spaide RF, Curcio CA. Anatomical correlates to the bands seen in the outer retina by optical coherence tomography: literature review and model. *Retina*. 2011;31:1609–1619.

19. Dubis AM, Costakos DM, Subramaniam CD, et al. Evaluation of normal human foveal development using optical coherence tomography and histologic examination. *Arch Ophthalmol*. 2012;130:1291–1300.

20. Vajzovic L, Hendrickson AE, O'Connell RV, et al. Maturation of the human fovea: correlation of spectral-domain optical coherence tomography findings with histology. *Am J Ophthalmol*. 2012;154:779–789, e2.

21. Lee H, Purohit R, Patel A, et al. In vivo foveal development using optical coherence tomography. *Invest Ophthalmol Vis Sci*. 2015;56:4537–4545.

22. Hendrickson AE, Yuodelis C. The morphological development of the human fovea. *Ophthalmology*. 1984;91:603–612.

23. Vinekar A, Avadhani K, Sivakumar M, et al. Understanding clinically undetected macular changes in early retinopathy of prematurity on spectral domain optical coherence tomography. *Invest Ophthalmol Vis Sci*. 2011;52:5183–5188.

24. Huynh SC, Wang XY, Rochtchina E, et al. Distribution of macular thickness by optical coherence tomography: findings from a population-based study of 6-year-old children. *Invest Ophthalmol Vis Sci*. 2006;47:2351–2357.

25. Gupta G, Donahue JP, You T. Profile of the retina by optical coherence tomography in the pediatric age group. *Am J Ophthalmol*. 2007;144:309–310.

26. El-Dairi MA, Asrani SG, Enyedi LB, et al. Optical coherence tomography in the eyes of normal children. *Arch Ophthalmol*. 2009;127:50–58.

27. Wang J, Spencer R, Leffler JN, et al. Characteristics of peripapillary retinal nerve fiber layer in preterm children. *Am J Ophthalmol*. 2012;153:850–855, e1.

28. Tong AY, El-Dairi M, Maldonado RS, et al. Evaluation of optic nerve development in preterm and term infants using handheld spectral-domain optical coherence tomography. *Ophthalmology*. 2014;121:1818–1826.

29. Yanni SE, Wang J, Cheng CS, et al. Normative reference ranges for the retinal nerve fiber layer, macula, and retinal layer thicknesses in children. *Am J Ophthalmol*. 2013;155: 354–360, e1.

30. Turk A, Ceylan OM, Arici C, et al. Evaluation of the nerve fiber layer and macula in the eyes of healthy children using spectral-domain optical coherence tomography. *Am J Ophthalmol*. 2012;153:552–559, e1.

31. Allingham MJ, Cabrera MT, O'Connell RV, et al. Racial variation in optic nerve head parameters quantified in healthy newborns by handheld spectral domain optical coherence tomography. *J AAPOS*. 2013;17:501–506.

32. Rothman AL, Sevilla MB, Freedman SF, et al. Assessment of retinal nerve fiber layer thickness in healthy, full-term neonates. *Am J Ophthalmol*. 2015;159:803–811.

33. Rothman AL, Sevilla MB, Mangalesh S, et al. Thinner retinal nerve fiber layer in very preterm versus term infants and

relationship to brain anatomy and neurodevelopment. *Am J Ophthalmol*. 2015;160:1296–1308, e2.

34. Gilbert C. Retinopathy of prematurity: a global perspective of the epidemics, population of babies at risk and implications for control. *Early Hum Dev*. 2008;84:77–82.

35. Isenberg SJ, Del Signore M, Chen A, et al. Corneal topography of neonates and infants. *Arch Ophthalmol*. 2004;122:1767–1771.

36. Fulton AB, Hansen RM, Moskowitz A, et al. Multifocal ERG in subjects with a history of retinopathy of prematurity. *Doc Ophthalmol*. 2005;111:7–13.

37. Barnaby AM, Hansen RM, Moskowitz A, et al. Development of scotopic visual thresholds in retinopathy of prematurity. *Invest Ophthalmol Vis Sci*. 2007;48:4854–4860.

38. Ecsedy M, Szamosi A, Karko C, et al. A comparison of macular structure imaged by optical coherence tomography in preterm and full-term children. *Invest Ophthalmol Vis Sci*. 2007;48:5207–5211.

39. Lago A, Matieli L, Gomes M, et al. Stratus optical coherence tomography findings in patients with retinopathy of prematurity. *Arq Bras Oftalmol*. 2007;70:19–21.

40. Hammer DX, Iftimia NV, Ferguson RD, et al. Foveal fine structure in retinopathy of prematurity: an adaptive optics Fourier domain optical coherence tomography study. *Invest Ophthalmol Vis Sci*. 2008;49:2061–2070.

41. Akerblom H, Larsson E, Eriksson U, et al. Central macular thickness is correlated with gestational age at birth in prematurely born children. *Br J Ophthalmol*. 2011;95:799–803.

42. Wu WC, Lin RI, Shih CP, et al. Visual acuity, optical components, and macular abnormalities in patients with a history of retinopathy of prematurity. *Ophthalmology*. 2012;119:1907–1916.

43. Recchia FM, Recchia CC. Foveal dysplasia evident by optical coherence tomography in patients with a history of retinopathy of prematurity. *Retina*. 2007;27:1221–1226.

44. Baker PS, Tasman W. Optical coherence tomography imaging of the fovea in retinopathy of prematurity. *Ophthalmic Surg Lasers Imaging*. 2010;41:201–206.

45. Park KA, Oh SY. Analysis of spectral-domain optical coherence tomography in preterm children: retinal layer thickness and choroidal thickness profiles. *Invest Ophthalmol Vis Sci*. 2012;53:7201–7207.

46. Tariq YM, Burlutsky G, Mitchell P. Macular parameters and prematurity: a spectral domain coherence tomography study. *J AAPOS*. 2012;16:382–385.

47. Wang J, Spencer R, Leffler JN, et al. Critical period for foveal fine structure in children with regressed retinopathy of prematurity. *Retina*. 2012;32:330–339.

48. Yanni SE, Wang J, Chan M, et al. Foveal avascular zone and foveal pit formation after preterm birth. *Br J Ophthalmol*. 2012;96:961–966.

49. Bonotto LB, Moreira AT, Bortolotto CM. Structural features of macular eyes of preschoolers born preterm: analysis by optical coherence tomography, and indirect ophthalmoscopy [in Portuguese]. *Arq Bras Oftalmol*. 2013;76:98–104.

50. Chrzanowska B, Szuminski M, Ozieblo-Kupczyk M, et al. Macular morphology and peripapillary retinal nerve fiber layer thickness in children with regressed retinopathy of prematurity [in Polish]. *Klin Oczna*. 2013;115:280–284.

51. Dubis AM, Subramaniam CD, Godara P, et al. Subclinical macular findings in infants screened for retinopathy of prematurity with spectral-domain optical coherence tomography. *Ophthalmology*. 2013;120:1665–1671.

52. Villegas VM, Capo H, Cavuoto K, et al. Foveal structure-function correlation in children with history of retinopathy of prematurity. *Am J Ophthalmol*. 2014;158:508–512, e2.

53. Pueyo V, Gonzalez I, Altemir I, et al. Microstructural changes in the retina related to prematurity. *Am J Ophthalmol*. 2015;159:797–802.

54. Rosen R, Sjostrand J, Nilsson M, et al. A methodological approach for evaluation of foveal immaturity after extremely preterm birth. *Ophthalmic Physiol Opt*. 2015;35:433–441.

55. Vajzovic L, Rothman AL, Tran-Viet D, et al. Delay in retinal photoreceptor development in very preterm compared to term infants. *Invest Ophthalmol Vis Sci*. 2015;56:908–913.

56. Akerblom H, Holmstrom G, Eriksson U, et al. Retinal nerve fibre layer thickness in school-aged prematurely-born children compared to children born at term. *Br J Ophthalmol*. 2012;96:956–960.

57. Park KA, Oh SY. Retinal nerve fiber layer thickness in prematurity is correlated with stage of retinopathy of prematurity. *Eye (Lond)*. 2015;9:1594–1602.

58. Moreno TA, O'Connell RV, Chiu SJ, et al. Choroid development and feasibility of choroidal imaging in the preterm and term infants utilizing SD-OCT. *Invest Ophthalmol Vis Sci*. 2013;54:4140–4147.

59. Wu WC, Shih CP, Wang NK, et al. Choroidal thickness in patients with a history of retinopathy of prematurity. *JAMA Ophthalmol*. 2013;131:1451–1458.

60. Anderson MF, Ramasamy B, Lythgoe DT, et al. Choroidal thickness in regressed retinopathy of prematurity. *Eye (Lond)*. 2014;28:1461–1468.

61. Cernichiaro-Espinosa LA, Garcia-Huerta MM, Giordano VE, et al. Comparison of iridocorneal angle in infants with retinopathy of prematurity and healthy infants using spectral domain optical coherence tomography. *J AAPOS*. 2014;18:344–346.

62. Lee AC, Maldonado RS, Sarin N, et al. Macular features from spectral-domain optical coherence tomography as an adjunct to indirect ophthalmoscopy in retinopathy of prematurity. *Retina*. 2011;31:1470–1482.

63. Joshi MM, Trese MT, Capone A Jr. Optical coherence tomography findings in stage 4A retinopathy of prematurity: a theory for visual variability. *Ophthalmology*. 2006;113:657–660.

64. Patel CK. Optical coherence tomography in the management of acute retinopathy of prematurity. *Am J Ophthalmol*. 2006;141:582–584.

65. Chavala SH, Farsiu S, Maldonado R, et al. Insights into advanced retinopathy of prematurity using handheld spectral domain optical coherence tomography imaging. *Ophthalmology*. 2009;116:2448–2456.

66. Muni RH, Kohly RP, Charonis AC, et al. Retinoschisis detected with handheld spectral-domain optical coherence tomography in neonates with advanced retinopathy of prematurity. *Arch Ophthalmol*. 2010;128:57–62.

67. Scott AW, Farsiu S, Enyedi LB, et al. Imaging the infant retina with a hand-held spectral-domain optical coherence tomography device. *Am J Ophthalmol*. 2009;147:364–373, e2.

68. Erol MK, Ozdemir O, Turgut Coban D, et al. Macular findings obtained by spectral domain optical coherence tomography in retinopathy of prematurity. *J Ophthalmol*. 2014;2014:468653.

69. Bondalapati S, Milam RW Jr, Ulrich JN, et al. The characteristics and short-term refractive error outcomes of cystoid macular edema in premature neonates as detected by spectral-domain optical coherence tomography. *Ophthalmic Surg Lasers Imaging*. 2015;46:806–812.

70. Rothman AL, Tran-Viet D, Gustafson KE, et al. Poorer neurodevelopmental outcomes associated with cystoid macular edema identified in preterm infants in the intensive care nursery. *Ophthalmology*. 2015;122:610–619.

71. Rothman AL, Tran-Viet D, Vajzovic L, et al. Functional outcomes of young infants with and without macular edema. *Retina*. 2015;35:2018–2027.

72. Vinekar A, Mangalesh S, Jayadev C, et al. Macular edema in Asian Indian premature infants with retinopathy of prematurity: impact on visual acuity and refractive status after 1-year. *Indian J Ophthalmol*. 2015;63:432–437.

73. Maldonado RS, Yuan E, Tran-Viet D, et al. Three-dimensional assessment of vascular and perivascular characteristics in subjects with retinopathy of prematurity. *Ophthalmology*. 2014;121:1289–1296.

74. Maldonado RS, O'Connell R, Ascher SB, et al. Spectral-domain optical coherence tomographic assessment of severity of cystoid macular edema in retinopathy of prematurity. *Arch Ophthalmol*. 2012;130:569–578.

75. Muni RH, Kohly RP, Sohn EH, et al. Hand-held spectral domain optical coherence tomography finding in shaken-baby syndrome. *Retina*. 2010;30:S45–S50.

76. Gerth C, Zawadzki RJ, Werner JS, et al. Retinal morphology in patients with BBS1 and BBS10 related Bardet-Biedl Syndrome evaluated by Fourier-domain optical coherence tomography. *Vision Res*. 2008;48:392–399.

77. Mano N, Mitsutsuji T, Yoshikawa Y, et al. Optical coherence tomography in an infant with Walker-Warburg syndrome. *Case Rep Ophthalmol*. 2015;6:210–215.

78. Gerth C, Zawadzki RJ, Werner JS, et al. Retinal morphological changes of patients with X-linked retinoschisis evaluated by Fourier-domain optical coherence tomography. *Arch Ophthalmol*. 2008;126:807–811.

79. Lee H, Sheth V, Bibi M, et al. Potential of handheld optical coherence tomography to determine cause of infantile nystagmus in children by using foveal morphology. *Ophthalmology*. 2013;120:2714–2724.

80. Lee H, Purohit R, Sheth V, et al. Retinal development in infants and young children with achromatopsia. *Ophthalmology*. 2015;122:2145–2147.

81. Lee H, Purohit R, Sheth V, et al. Retinal development in albinism: a prospective study using optical coherence tomography in infants and young children. *Lancet*. 2015; 385(suppl 1):S14.

82. Huot CS, Desai KB, Shah VA. Spectral domain optical coherence tomography of combined hamartoma of the retina and retinal pigment epithelium. *Ophthalmic Surg Lasers Imaging*. 2009;40:322–324.

83. Vinekar A, Quiram P, Sund N, et al. Plasmin-assisted vitrectomy for bilateral combined hamartoma of the retina and retinal pigment epithelium: histopathology, immunohistochemistry, and optical coherence tomography. *Retin Cases Brief Rep*. 2009;3:186–189.

84. Goel N, Pangtey B, Bhushan G, et al. Spectral-domain optical coherence tomography of astrocytic hamartomas in tuberous sclerosis. *Int Ophthalmol*. 2012;32:491–493.

85. Xu L, Burke TR, Greenberg JP, et al. Infrared imaging and optical coherence tomography reveal early-stage astrocytic hamartomas not detectable by fundoscopy. *Am J Ophthalmol*. 2012;153:883–889, e2.

86. Kang HM, Koh HJ, Chung EJ. Spectral-domain optical coherence tomography of combined hamartoma of the retina and retinal pigment epithelium in neurofibromatosis. *Korean J Ophthalmol*. 2013;27:68–71.

87. Takahashi A, Ooto S, Yoshimura N. High-penetration optical coherence tomography and enhanced depth imaging in presumed retinal pigment epithelial hamartoma. *Retin Cases Brief Rep*. 2013;7:179–182.

88. Cao C, Markovitz M, Ferenczy S, et al. Hand-held spectral-domain optical coherence tomography of small macular retinoblastoma in infants before and after chemotherapy. *J Pediatr Ophthalmol Strabismus*. 2014;51:230–234.

89. Chidambara L, Jayadev C, Mangalesh S, et al. Correlation of spectral-domain optical coherence tomography with fundus fluorescein angiography in an infant with retinal hamartomas. *Eur J Ophthalmol*. 2015;25:e106–e108.

90. Yousef YA, Shroff M, Halliday W, et al. Detection of optic nerve disease in retinoblastoma by use of spectral domain optical coherence tomography. *J AAPOS*. 2012;16:481–483.

91. Jiramongkolchai K, Freedman SF, El-Dairi MA. Retinal changes in pediatric glaucoma and nonglaucomatous optic atrophy. *Am J Ophthalmol*. 2015;161:188–195, e1.

92. El-Dairi MA, Holgado S, Asrani SG, et al. Correlation between optical coherence tomography and glaucomatous optic nerve head damage in children. *Br J Ophthalmol*. 2009;93:1325–1330.

93. Ely AL, El-Dairi MA, Freedman SF. Cupping reversal in pediatric glaucoma–evaluation of the retinal nerve fiber layer and visual field. *Am J Ophthalmol*. 2014;158:905–915.

94. Abramov I, Gordon J, Hendrickson A, et al. The retina of the newborn human infant. *Science*. 1982;217:265–267.

95. Pilat A, Sibley D, McLean RJ, et al. High-resolution imaging of the optic nerve and retina in optic nerve hypoplasia. *Ophthalmology*. 2015;122:1330–1339.

96. Avery RA, Hwang EI, Ishikawa H, et al. Handheld optical coherence tomography during sedation in young children with optic pathway gliomas. *JAMA Ophthalmol*. 2014;132: 265–271.

97. Avery RA, Cnaan A, Schuman JS, et al. Reproducibility of circumpapillary retinal nerve fiber layer measurements using handheld optical coherence tomography in sedated children. *Am J Ophthalmol*. 2014;158:780–787, e1.

98. Gu S, Glaug N, Cnaan A, et al. Ganglion cell layer-inner plexiform layer thickness and vision loss in young children with optic pathway gliomas. *Invest Ophthalmol Vis Sci*. 2014;55:1402–1408.

99. El-Dairi MA, Holgado S, O'Donnell T, et al. Optical coherence tomography as a tool for monitoring pediatric pseudotumor cerebri. *J AAPOS*. 2007;11:564–570.

100. Gospe SM III, Bhatti MT, El-Dairi MA. Anatomic and visual function outcomes in paediatric idiopathic intracranial hypertension. *Br J Ophthalmol*. 2015;100:505–509.

101. El-Dairi MA, Holgado S, O'Donnell T, et al. Optical coherence tomography as a tool for monitoring pediatric pseudotumor cerebri. *J AAPOS*. 2007;11:564–570.